



## PAPER

## Magnetic phases of orbital bipartite optical lattices

Pil Saugmann and Jonas Larson

Department of Physics, Stockholm University, AlbaNova University Center, SE-106 91 Stockholm, Sweden

E-mail: [pilmaria.saugmann@fysik.su.se](mailto:pilmaria.saugmann@fysik.su.se)**Keywords:** cold atoms, optical lattice, phase diagram, quantum simulation, magnetic models

## OPEN ACCESS

RECEIVED  
14 June 2019REVISED  
13 January 2020ACCEPTED FOR PUBLICATION  
16 January 2020PUBLISHED  
11 February 2020

Original content from this work may be used under the terms of the [Creative Commons Attribution 4.0 licence](#).

Any further distribution of this work must maintain attribution to the author(s) and the title of the work, journal citation and DOI.



## Abstract

In the Hamburg cold atom experiment with orbital states in an optical lattice, *s*- and *p*-orbital atomic states hybridize between neighboring sites. In this work we show how this alternation of sites hosting *s*- and *p*-orbital states gives rise to a plethora of different magnetic phases, quantum and classical. We focus on phases whose properties derive from frustration originating from a competition between nearest and next nearest neighboring exchange interactions. The physics of the Mott insulating phase with unit filling is described by an effective spin-1/2 Hamiltonian showing great similarities with the  $J_1$ - $J_2$  model. Based on the knowledge of the  $J_1$ - $J_2$  model, supported by numerical simulations, we discuss the possibility of a quantum spin liquid phase in the present optical lattice system. In the superfluid regime we consider the parameter regime where the *s*-orbital states can be adiabatically eliminated to give an effective model for the *p*-orbital atoms. At the mean-field level we derive a generalized classical XY model, and show that it may support maximum frustration. When quantum fluctuations can be disregarded, the ground state should be a spin glass.

## 1. Introduction

Ultracold atoms trapped in optical lattices has within the last two decades evolved into a efficient tool for studying strongly interacting quantum many-body systems [1]. The systems allow for explorations of a variety of lattice models, in terms of changing lattice geometries, varying parameter strengths and initialize desired states. Put together with the possibility to perform high fidelity state measurements, they are the perfect candidates for quantum simulators [2]. Real physical systems that can solve quantum mechanical problems intractable on classical computers.

From a condensed matter physics viewpoint, the Hubbard models [3] are known to be prime candidates to be simulated. Theoretically proposed in [4], and followed by the experimental realization of the Bose–Hubbard Mott–superfluid phase transition (PT) by Greiner *et al* [5], an avalanche of activity started. Due to the importance in other branches of condensed matter physics, it did not take long until orbital physics was discussed in terms of cold atoms in optical lattices [6, 7].

It was suggested that internal atomic hyperfine levels could be used to mimic models of quantum magnetism [8]. Another way to mimic quantum magnetism is to make use of internal orbital states instead [9]. Internal orbital states was first studied, in the context of ultra cold atoms, by Isacsson and Girvin [6]. They showed that the superfluid (SF) state of a *p*-orbital Bose–Hubbard model on a square optical lattice arranges in a vortex lattice, which breaks time-reversal symmetry and have a complex order parameter [6]. The life-time of these excited states is long, which was later confirmed experimentally [10]. For bosonic atoms, the main loss mechanism is the scattering of two *p*-orbital atoms into one *s* and one *d* orbital atom. To avoid this, superlattices can be employed where such scattering processes are far off-resonant. A few years latter came the first experiment that studied different magnetic phases [11], and thereby also the corresponding quantum PTs.

Quantum magnetism becomes especially interesting in the case of *frustration*. Here spin liquids and glasses are phases which can emerge from strong frustration. The classical counterparts typically implies a large number of classically degenerate ground states [12], and at sufficiently low temperatures quantum spin liquids (QSLs) [13] can be formed. These phases are expected to host many novel properties like topological

fractional excitations [14]. They are experimentally very elusive and only indirect measurements that suggest the presence of QSL have been found [13] so far. In cold atoms in optical lattices, ‘lattice shaking’ techniques can be used to adjust the tunneling terms, and this led to observation of magnetic frustration [15]. The experiment only demonstrates classical frustration, but it predicts the existence of QSL states in the same type of system set-up [16].

One cold atomic system which may host frustration in its groundstates, is the Hamburg experiment of Hemmerich [17, 18]; degenerate  $s$ - and  $p$ -orbital atoms hybridize on neighboring sites in a superlattice. Also for this configuration the SF phase consists of vortices leading to a complex order parameter [19], and it was further argued that thermal fluctuations will induce a new phase, a chiral Bose liquid, in this model [20]. Nevertheless, much of the phase diagram of both the insulating and superfluid phase of the Hamburg set-up remains unexplored.

In the insulating phase, the sites hosting  $s$ -orbitals effectively mediate the coupling between sites with  $p$ -orbital atoms. An effective model emerges consisting only of  $p$ -orbital atoms where the strength of the coupling between nearest neighbors (NN) is of the same order as the coupling strength between next-nearest neighbors (NNN). This can make it possible to achieve strong frustration [13] and hence hope of realizing a QSL phases. The resulting model resembles the  $J_1$ – $J_2$  model that has served as a work horse in the study of QSL’s. Using mean-field methods and exact diagonalization we see evidence for a novel phase that agrees with earlier predictions of a QSL in the  $J_1$ – $J_2$  model.

In the SF phase, the  $s$ -orbital atoms cannot be eliminated with the same argument due to onsite particle fluctuations. Instead, when the  $s$ - and  $p$ -orbitals are far detuned in energy the  $s$ -atoms can be adiabatically eliminated and an effective model for the  $p$ -atoms is derived. As for the insulating phase, the resulting model has both NN and NNN interactions, where the sign of the detuning determines the sign of the tunneling strengths. For negative tunneling strengths the SF arrange in a phase with alternating vortices and anti-vortices on neighboring sites, i.e. again breaking time-reversal symmetry and with a complex order parameter. For positive tunneling strengths the system shows frustrations, and at the mean-field level we derive a generalization of a classical XY model that has been a prototype model for exploring classical frustration and spin liquid phases. We find support for a frustration-driven phase also in our model which presumably is a spin liquid.

## 2. Model Hamiltonian

### 2.1. Physical system and its Hamiltonian

The optical potential of the Hamburg experiment [17, 18] forms two sublattices,  $\mathcal{S}$  and  $\mathcal{P}$  with the  $\mathcal{P}$ -sites deeper, see figure 1(a). By tuning the lattice parameters, the relative depth is chosen such that the two  $p_x$ - and  $p_y$ -orbitals are quasi resonant with the  $s$ -orbitals (figure 1(c)). The atoms are assumed to only populate these three bands. We neglect any losses to other bands, and consider the *tight-binding approximation*, consisting in only taking NN tunneling and onsite  $s$ -wave scattering into account.

The  $p_x$ - and  $p_y$ -orbital states have, respectively, a node in the  $x$ - and  $y$ -direction—as shown in figure 1(b), while the  $s$ -orbitals are polar symmetric. In the bipartite lattice, the tunneling is between  $\mathcal{S}$ - and  $\mathcal{P}$ -sites and is such that the tunneling in the  $\alpha$ -direction ( $\alpha = x, y$ ) is possible only for a  $p_\alpha$ -orbital atom due to the parity of the orbital states together with the shape of the potential. There are two ways for the  $p_x$ - and  $p_y$ -orbital atoms to couple; a  $p_x$ -orbital atom can tunnel to an  $s$ -orbital atom which then tunnels to a  $p_y$ -orbital atom, or two  $p_x$ -orbital atoms can scatter into two  $p_y$ -orbital atoms or vice versa.

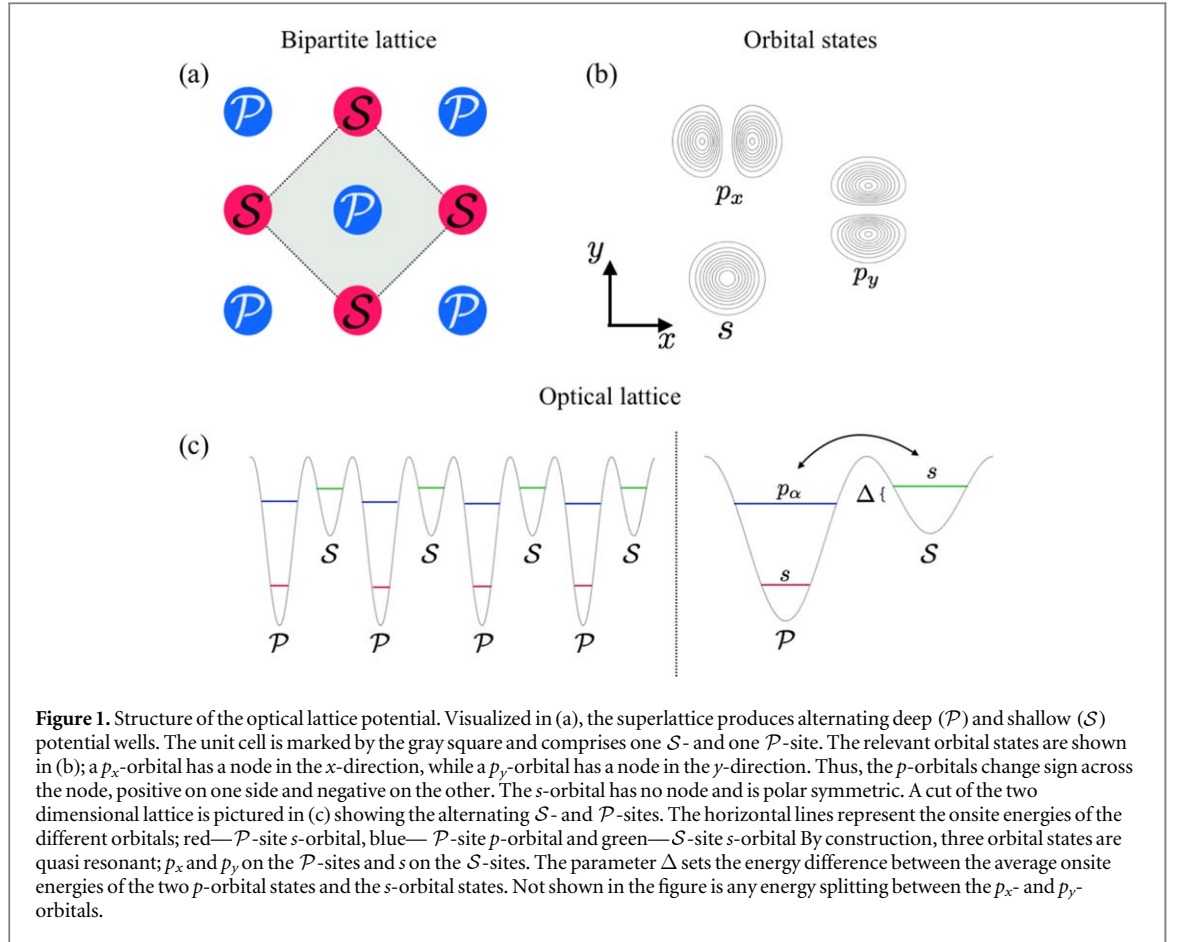
We use the notation  $\hat{a}_{\alpha\mathbf{i}}$  ( $\alpha = s, x, y$ ) for the bosonic annihilation operators. The subscript  $\mathbf{i} = (i_x, i_y)$  refers to the site, in general we use the subscript  $\mathbf{i}$  and  $\mathbf{j}$  for the  $\mathcal{S}$ - and  $\mathcal{P}$ -sites respectively. When restricting the model to these three bands, an atomic operator annihilating an atom at  $\mathbf{x} = (x, y)$  is expanded as

$$\hat{\Psi}(\mathbf{x}) = \sum_{\mathbf{i} \in \mathcal{S}} \hat{a}_{s\mathbf{i}} w_{s\mathbf{i}}(\mathbf{x}) + \sum_{\alpha} \sum_{\mathbf{j} \in \mathcal{P}} \hat{a}_{\alpha\mathbf{j}} w_{\alpha\mathbf{j}}(\mathbf{x}), \quad (1)$$

where  $w_{s\mathbf{i}}(\mathbf{x})$  and  $w_{\alpha\mathbf{j}}(\mathbf{x})$  are the corresponding Wannier functions localized at site  $\mathbf{i}$  and  $\mathbf{j}$ .

In the isotropic lattice,  $t_x = t_y > 0$ , while for anisotropic lattices these equalities are not strict, and the two  $p$ -orbital states are not degenerate. The onsite energy difference between the two orbitals is  $\delta$  and with the zero energy chosen exactly between the two states. The kinetic term in the Hamiltonian  $\hat{H} = \hat{H}_{\text{kin}} + \hat{H}_{\text{int}}$  is

$$\begin{aligned} \hat{H}_{\text{kin}} = & -t_x \sum_{\langle \mathbf{ij} \rangle_x} (\hat{a}_{s\mathbf{i}}^\dagger \hat{a}_{x\mathbf{j}} + \text{h.c.}) \\ & -t_y \sum_{\langle \mathbf{ij} \rangle_y} (\hat{a}_{s\mathbf{i}}^\dagger \hat{a}_{y\mathbf{j}} + \text{h.c.}) + \Delta \sum_{\mathbf{i}} \hat{n}_{s\mathbf{i}} + \frac{\delta}{2} \sum_{\mathbf{j}} (\hat{n}_{x\mathbf{j}} - \hat{n}_{y\mathbf{j}}), \end{aligned} \quad (2)$$



while the interaction term  $\hat{H}_{\text{int}} = \hat{H}_{nn} + \hat{H}_{\text{fc}}$  is further decomposed into ‘density–density’ interactions

$$\hat{H}_{nn} = \sum_{\alpha} \sum_{j \in \mathcal{P}} \frac{U_{\alpha\alpha}}{2} \hat{n}_{\alpha j} (\hat{n}_{\alpha j} - 1) + \sum_{i \in \mathcal{S}} \frac{U_{ss}}{2} \hat{n}_{si} (\hat{n}_{si} - 1) + \sum_{\alpha\beta, \alpha \neq \beta} \sum_{j \in \mathcal{P}} U_{\alpha\beta} \hat{n}_{\alpha j} \hat{n}_{\beta j} \quad (3)$$

and ‘flavor-changing’ interactions

$$\hat{H}_{\text{fc}} = \sum_{\alpha\beta, \alpha \neq \beta} \sum_{j \in \mathcal{P}} \frac{U_{\alpha\beta}}{2} (\hat{a}_{\alpha j}^{\dagger} \hat{a}_{\alpha j}^{\dagger} \hat{a}_{\beta j} \hat{a}_{\beta j} + \text{h.c.}). \quad (4)$$

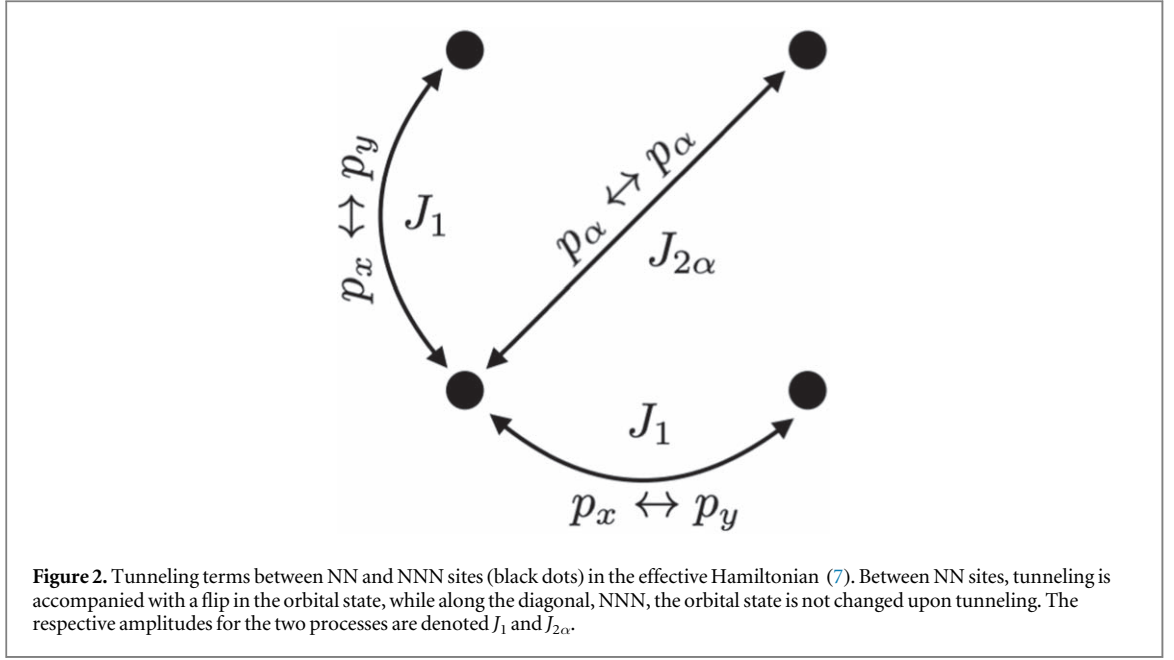
Here,  $\langle \dots \rangle_{\alpha}$  is the summation over NN in the  $\alpha$ -direction. The operators  $\hat{n}_{\alpha j} = \hat{a}_{\alpha j}^{\dagger} \hat{a}_{\alpha j}$  and  $\hat{n}_{si} = \hat{a}_{si}^{\dagger} \hat{a}_{si}$  give the number of orbital atoms on the specific site. With  $p_x/p_y$ -orbitals having an onsite energy  $\pm\delta/2$ , the onsite energy for the  $s$ -orbitals is  $\Delta$ . The interaction terms alone supports a  $\mathbb{Z}_2$ -parity symmetry that represents conservation of orbital atoms modulo 2. This symmetry is broken as  $p$ -orbital atoms can tunnel into  $s$ -orbital atoms. In the isotropic lattice with  $\delta = 0$  there is  $\mathbb{Z}_4$  symmetry, corresponding to 90 degree rotations for the full many-body Hamiltonian. This corresponds to swapping the  $p_x$ - and  $p_y$ -orbitals and rotate the axes. When the lattice is anisotropic this symmetry breaks down into a  $\mathbb{Z}_2$  represented by a 180 degree rotation. The total particle number is a preserved quantity, and it is this continuous  $U(1)$  symmetry that is broken across the Mott-SF PT [21]. The onsite energies  $\delta$  and  $\Delta$ , the relative interaction strengths  $U_{\alpha\beta}$  and the tunneling amplitudes  $t_{\alpha}$  are all determined by the overlap integrals of the Wannier functions. For example, the interaction strengths are

$$U_{\alpha\beta} = U_0 \int d\mathbf{x} |w_{\alpha j}(\mathbf{x})|^2 |w_{\beta j}(\mathbf{x})|^2, \quad U_{ss} = U_0 \int d\mathbf{x} |w_{sj}(\mathbf{x})|^4, \quad (5)$$

where  $U_0$  is a constant proportional to the  $s$ -wave scattering length. In the harmonic approximation, the Wannier functions are replaced with harmonic functions, e.g. (in dimensionless units)

$$w_{xj}(\mathbf{x}) = \left( \frac{1}{\pi\sigma^2} \right)^{1/2} (x - x_{j_x}) \exp \left( -\frac{(x - x_{j_x})^2}{2\sigma^2} - \frac{(y - y_{j_y})^2}{2\sigma^2} \right), \quad (6)$$

where  $(x_{j_x}, y_{j_y})$  is the position of site  $\mathbf{j} = (j_x, j_y)$ , and we have assumed the width  $\sigma$  to be the same in the  $x$ - and  $y$ -directions. The interaction strengths then obey  $U_{xx} = U_{yy} = 3U_{xy}$  [22]. The  $U_{ss}$  is not simply related to the other interaction parameters since it derives from the interaction in an  $\mathcal{S}$ - and not a  $\mathcal{P}$ -site, but it is of the same order as  $U_{\alpha\alpha}$ .



## 2.2. Large detuning effective model

When the energy off-set  $\Delta$  between  $p$ - and  $s$ -orbital states is small, the two types of atomic states hybridize to build up the full system state [21]. When  $|\Delta|$  is the large parameter, compared to the  $t_\alpha$ 's and to  $U_{ss}$ , population transfer between the  $\mathcal{S}$ - and the  $\mathcal{P}$ -sites is suppressed due to the large energy difference. The kinetics is still not trivial, as the intermediate states can virtually mediate both NN and NNN tunneling in a two-step process.

The derivation of the effective model that results from the elimination of the  $s$ -orbitals is given in appendix A. The resulting Hamiltonian reads

$$\begin{aligned} \hat{H}_{\text{eff}}^{(\Delta)} = & - \sum_{\alpha} \sum_{\langle ij \rangle_{\alpha}} J_{2\alpha} \hat{a}_{\alpha i}^{\dagger} \hat{a}_{\alpha j} - J_1 \sum_{\alpha\beta, \alpha \neq \beta} \sum_{\langle ij \rangle} (\hat{a}_{\alpha i}^{\dagger} \hat{a}_{\beta j} + \text{h.c.}) \\ & - \sum_{\alpha} \sum_j J_{2\alpha} \hat{n}_{\alpha j} + \frac{\delta}{2} \sum_j (\hat{n}_{xj} - \hat{n}_{yj}) + \sum_{\alpha} \sum_j \frac{U_{\alpha\alpha}}{2} \hat{n}_{\alpha j} (\hat{n}_{\alpha j} - 1) \\ & + \sum_{\alpha\beta, \alpha \neq \beta} \sum_j U_{\alpha\beta} \hat{n}_{\alpha j} \hat{n}_{\beta j} + \sum_{\alpha\beta, \alpha \neq \beta} \sum_j \frac{U_{\alpha\beta}}{2} (\hat{a}_{\alpha j}^{\dagger} \hat{a}_{\alpha j}^{\dagger} \hat{a}_{\beta j} \hat{a}_{\beta j} + \text{h.c.}), \end{aligned} \quad (7)$$

where  $J_{2\alpha} = |t_{\alpha}|^2 / \Delta$  and  $J_1 = t_x t_y / \Delta$  give the tunneling amplitudes along NN and NNN's respectively, see figure 2. The two tunneling strengths are of the same order, e.g. in an isotropic lattice,  $t_x = t_y$  and  $J_{2x} = J_{2y} = J_1 \equiv J$ . What is appealing is that the signs of the tunneling is adjustable by changing the sign of  $\Delta$ . NN tunneling induces a flavor-changing of the orbital state, which can be seen as an effective spin–orbit coupling [23]. The third sum represents ‘Stark shifts’ due to virtual couplings to the  $s$ -orbitals.

## 2.3. Large interaction effective model

In the insulating phases we expand in  $t/U$ , and project on to the Mott insulating phase with one atom per lattice site [24]. The flavor-changing interaction term (4) is non-diagonal in the Fock basis and causes the allowed processes in the perturbation expansion to be much richer. Since  $p$ -orbital atoms are only allowed to tunnel in the direction of its node, the second order terms are then trivial. Take a  $p_x$ -orbital atom, it can tunnel to its neighboring  $s$ -site with amplitude  $t_x$  giving an interaction contribution  $\sim 1/U_{ss}$ , and then one  $s$ -orbital atom tunnels back to the empty  $p$ -site as a  $p_x$ -orbital atom and again with an amplitude  $t_x$ . This is nothing but an onsite energy shift. Thus, via second order processes it is not possible to generate effective interaction terms between the orbitals, so to reach a non trivial effective Hamiltonian one must include fourth order terms as well. This gives rise to NN and NNN couplings for the  $\mathcal{P}$ -sites. As there is no internal degree-of-freedom in the  $\mathcal{S}$ -sites, these will effectively freeze out. There are essential two different types of tunneling processes, non-loops and loops, in the non-loop process the atom tunnels out and back along the same path which is not the case in the loop processes. The non-loop processes give rise to a density–density coupling, while the loop processes render orbital swapping couplings. The NNN couplings consist only of non-loop processes, while the NN couplings have both non-loop and loop contributions.

Restricting to single particle occupancy on each site and defining the *Schwinger spin bosons* [24]

$$\begin{aligned}\hat{S}_i^Z &= \frac{1}{2}(\hat{a}_{xi}^\dagger \hat{a}_{xi} - \hat{a}_{yi}^\dagger \hat{a}_{yi}), \\ \hat{S}_i^+ &= \hat{S}_i^X + i\hat{S}_i^Y = \hat{a}_{xi}^\dagger \hat{a}_{yi}, \\ \hat{S}_i^- &= \hat{S}_i^X - i\hat{S}_i^Y = \hat{a}_{yi}^\dagger \hat{a}_{xi},\end{aligned}\quad (8)$$

the Hamiltonian is mapped onto one of spin-1/2 particles

$$\hat{H}_{\text{eff}} = h \sum_i \hat{S}_i^Z + J_2^Z \sum_{\langle ij \rangle} \hat{S}_i^Z \hat{S}_j^Z + J_1^Z \sum_{\langle ij \rangle} \hat{S}_i^Z \hat{S}_j^Z + \sum_{\langle ij \rangle} J_1^X \hat{S}_i^X \hat{S}_j^X + J_1^Y \hat{S}_i^Y \hat{S}_j^Y. \quad (9)$$

The first sum is a field in the Z-direction with an amplitude  $h$  [9], the subscripts on the coupling amplitudes indicate whether the sum is over NN (1) or NNN (2) sites. The explicit expressions for the coupling amplitudes are presented in the appendix B, and here we only point out the relation  $J_1^Z = -J_2^Z/2$ . Without the second term over NNN the model comprises the two dimensional XYZ model [25].

### 3. Phase diagrams

For bosonic atoms in a bipartite  $s$ - $p$  lattice, the Mott insulator-SF phase boundaries as well as general properties of the SF phase were studied in [21] using the Gutzwiller mean-field method. However, the non-zero detuning  $\Delta \neq 0$  situation has been unnoticed, and furthermore for the insulating phases most of the physics is still unexplored.

#### 3.1. Superfluid phase diagram

Deep in the SF phase quantum fluctuations play such a small role that they can be neglected, and we can apply the simplest mean-field approximation where we assign a coherent state to every boson mode [26]. Thus, the full state can be expressed as

$$|\Psi\rangle = \prod_{i \in \mathcal{S}} |\alpha_{si}\rangle_i \prod_{j \in \mathcal{P}} |\alpha_{xj}, \alpha_{yj}\rangle_j, \quad (10)$$

where  $\hat{a}_{si}|\alpha_{si}\rangle_i = \alpha_{si}|\alpha_{si}\rangle_i$  and equivalently for the  $x$ - and  $y$ -modes. The full condensate order parameter becomes

$$\Psi(x) = \sum_{i \in \mathcal{S}} \alpha_{si} w_{si}(\mathbf{x}) + \sum_{j \in \mathcal{P}} [\alpha_{xj} w_{xj}(\mathbf{x}) + \alpha_{yj} w_{yj}(\mathbf{x})]. \quad (11)$$

The complex coherent state amplitudes are determined from minimizing the energy functional  $E[\alpha_{si}, \alpha_{xj}, \alpha_{yj}] = \langle \Psi | \hat{H} | \Psi \rangle$ . The energy functional is found by replacing the boson operators with their coherent state amplitudes, e.g.  $\hat{a}_{si} \rightarrow \alpha_{si}$ . The absolute value squared of the complex amplitudes give the onsite atom numbers, e.g.  $n_{si} = |\alpha_{si}|^2$ , while the onsite phases (e.g.  $\alpha_{si} = \sqrt{n_{si}} \exp(i\phi_{si})$ ) determine the global condensate coherence.

##### 3.1.1. Large detuning phase diagram

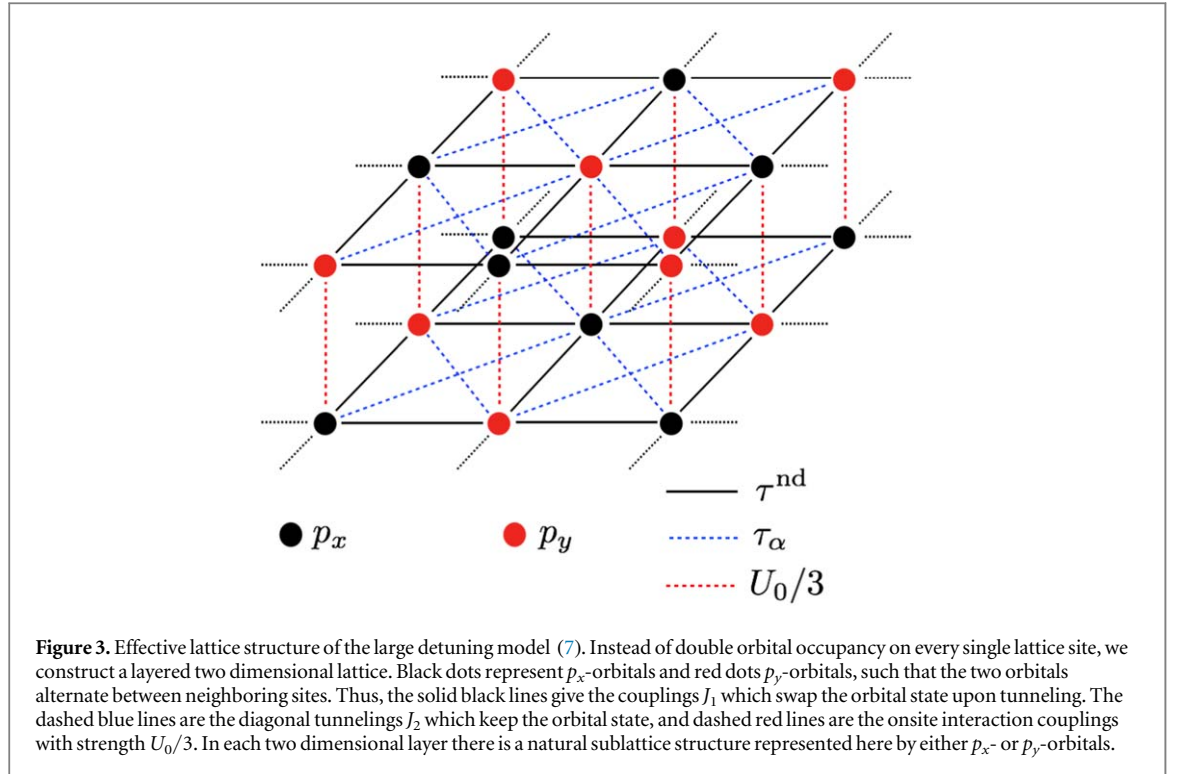
The  $\Delta = 0$  situation was explored experimentally in [17] and theoretically in [21]. Therefore, here we only consider the large detuning case, with the Hamiltonian given by equation (7).

When minimizing the energy functional with respect to the mean-field parameters, provided that  $\delta = 0$  one finds that the densities of the two orbitals are equal,  $n_{xj} = n_{yj} \equiv n$ . This is expected, but we may note that in higher dimensions this symmetry may be spontaneously broken [22]. In the polar representation,  $\alpha_{xj} = \sqrt{n_{xj}} \exp(i\phi_{xj})$  and  $\alpha_{yj} = \sqrt{n_{yj}} \exp(i\phi_{yj})$ , the energy depends on the angles and the global density  $n$  which we set to unity. For now we assume the isotropic lattice, i.e.  $\delta = 0$  and  $J_{2x} = J_{2y} \equiv J_2$ , and when omitting constant terms the mean-field energy becomes

$$\begin{aligned}E_{\text{MF}}[\phi_{\alpha j}] &= -2J_2 \sum_{\alpha} \sum_{\langle ij \rangle} \cos(\phi_{\alpha i} - \phi_{\alpha j}) - 2J_1 \sum_{\alpha, \beta, \alpha \neq \beta} \sum_{\langle ij \rangle} \cos(\phi_{\alpha i} - \phi_{\beta j}) \\ &\quad + \frac{U_0}{3} \sum_j \cos(2(\phi_{xj} - \phi_{yj})).\end{aligned}\quad (12)$$

This is a two-flavor *rotor model* or classical XY model [27], i.e. on each site sit two classical rotors  $s_{\alpha j} = (\sin \phi_{\alpha j}, \cos \phi_{\alpha j})$  which couple onsite to one another with  $U_0/3$  and between sites with  $2J_1$  or  $2J_2$ . For the isotropic lattice we have  $J_1 = J_2$ , which is the point of frustration in our model<sup>1</sup>. It is convenient to introduce an

<sup>1</sup> Recall that in our model the maximum frustration point is  $J_1 = J_2$ , and not  $J_1 = 2J_2$  as in the classical  $J_1$ - $J_1$  model.



effective lattice for our model where every site hosts instead a single orbital (rotor). This is pictured in figure 3; we get two layers and on each plane the onsite states alternate between  $p_x$  and  $p_y$ . The flavor-changing interaction couples the two layers.

With vanishing interaction,  $U_0 = 0$  we regain two copies of classical XY models with NN and NNN exchange interactions. In general, the competition between such terms may give rise to novel phases and phenomena like *charge density waves* [28], *supersolids* [29] and frustration [30–32]. The study of frustration in classical XY models on square lattices has a long history [33–35]. It may emerge even for NN models on a square lattice provided the tunneling coefficients  $\tau_i^j$  on a single plaquette obey a gauge rule mimicking a magnetic flux penetrating every plaquette. The unfrustrated regular XY model has zero flux, while the greatest frustration is obtained for half a flux quanta and has been termed *fully frustrated XY* or the *Villain model* [34]. When the two anti-ferromagnetic NN and NNN exchange interactions compete, frustration also occurs [30–32, 36–38]. When the NN coupling vanishes the model decouples into two square lattices and the ground state consists of two independent Néel states in the two sublattices. When instead the NNN coupling is zero, the ground state is a Néel state extended over the full lattice. When both couplings are non-zero there is no solution that simultaneously fulfill anti-ferromagnetic order on both sublattices and the full lattice. While the structure of the finite temperature phase diagram is still under debate [39], the  $T = 0$  phase diagram is known [40]. For  $J_1 < 2J_2$ , quantum fluctuations lift the degeneracy of the ground state and cause long range order, the *order-by-disorder* mechanism [41]. It was shown, using spin wave theory, that these fluctuations order the state such that the anti-ferromagnets in the two sublattices become collinear—*striped phase*, i.e. the relative phase between two neighboring sites is either 0 or  $\pi$  [30]. For  $J_1 > 2J_2$ , anti-ferromagnetic order is established in the full lattice—*Néel phase*. At the frustration point, a glass phase appears, and due to the chiral symmetry the ground state is doubly degenerate. taking quantum fluctuations into account, a possible state is a spin liquid phase that survives in the vicinity of the frustration point [38]. A large- $N$  expansion indicated that such a spin liquid phase should, however, only exist at exactly the symmetry point [37].

The fully frustrated XY model is especially interesting due to the spin glass phase existing despite lack of any disorder that manifestly breaks translational symmetry [33, 35]. For the Villain model, the nature of the transition from a disordered to a glass phase has been thoroughly discussed. The continuous symmetry cannot be spontaneously broken according to the *Mermin–Wagner theorem* [24], and the corresponding transition should instead be of the *Kosterlitz–Thouless* type. However, the discrete  $\mathbb{Z}_2$ -symmetry can indeed be spontaneously broken and could give rise to an Ising type transition [42]. Three scenarios emerge; whether (i) it is a Kosterlitz–Thouless transition followed by an Ising one, (ii) a mixture of the two occurring simultaneously for the same critical temperature, or (iii) a transition belonging to a new universality class, see [35]. The consensus seem to be alternative (i). It has been further argued that the state of the system in the narrow window between the two transitions is a chiral spin liquid [43, 44].

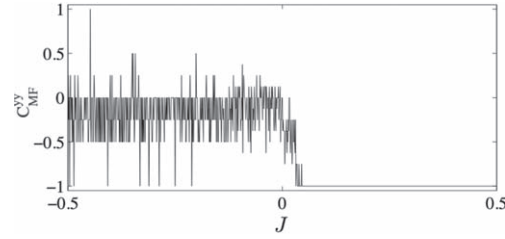


**Figure 4.** The mean-field correlator  $C_{\text{MF}}^{\text{YY}}$  of equation (15) as a function of the coupling  $J$ , ranging from negative to positive values. The lattice is considered isotropic and for the numerics we have used a  $4 \times 4$  lattice with periodic boundary conditions, and furthermore we have set  $U_0 = 1$ . For positive tunneling amplitudes  $J$  the system orders in an anti-ferromagnetic phase marked by  $C_{\text{MF}}^{\text{YY}} = -1$ . However, when we cross over to negative  $J$  the correlator starts to fluctuate greatly from one  $J$ -value to the next. Such fluctuations signals that there are several mean-field solutions with roughly the same energy and the numerical algorithm randomly picks one of them.

We verify the presence of frustration in our model by numerically extract the ground state for a  $4 \times 4$  lattice. The anti-ferromagnetic order obtained when  $J > 0$  is reflected in the NN ( $|\mathbf{i} - \mathbf{j}| = 1$ ) correlator

$$C^{\text{YY}}(\mathbf{i}, \mathbf{j}) = \langle \hat{S}_i^Y \hat{S}_j^Y \rangle. \quad (13)$$

In the mean-field approximation we have

$$C_{\text{MF}}^{\text{YY}}(\mathbf{i}, \mathbf{j}) = \sin(\phi_{xj} - \phi_{yj}) \sin(\phi_{xi} - \phi_{yi}), \quad (14)$$

which for the anti-ferromagnetic phase becomes  $C_{\text{MF}}^{\text{YY}}(\mathbf{i}, \mathbf{j}) = -1$ . We can go on and define the average correlator

$$C_{\text{MF}}^{\text{YY}} = \frac{1}{2N} \sum_{\langle \mathbf{i}, \mathbf{j} \rangle} C_{\text{MF}}^{\text{YY}}(\mathbf{i}, \mathbf{j}), \quad (15)$$

where  $N$  is the total number of sites, and the sum is over all NN bonds in the full lattice. It is clear that  $-1 \leq C_{\text{MF}}^{\text{YY}} \leq +1$  with  $C_{\text{MF}}^{\text{YY}} = -1$  for the anti-ferromagnetic phase and  $C_{\text{MF}}^{\text{YY}} = +1$  for the ferromagnetic phase. In figure 4 the numerical results for the correlator  $C_{\text{MF}}^{\text{YY}}$  show how it depends on the coupling  $J$  ( $=J_1 = J_2$ ). At positive couplings we verify the analytically predicted anti-ferromagnetic order which, apart from numerical fluctuations, exists down to  $J = 0$ . For negative  $J$  the numerics show large fluctuations from one simulation to the next meaning that the numerical minimization algorithm finds very different ground states. This is a smoking gun of classical frustration.

In the experiments [17, 18], with  $\Delta = 0$ , the order of the condensate were determined in a time-of-flight measurement. The detection verified a complex order parameter and thereby a broken time-reversal symmetry. In the model considered here with a large detuning  $\Delta$ , the same type of measurement will give fingerprints of the phases. The ferromagnetic case should produce similar time-of-flight images as in [17, 18], while in the frustrated case the images will look very different due to the more irregular global phase order of the condensate.

### 3.2. Mott insulating phase diagram

In the insulating phase the Hamiltonian on the form of (9) is part of a larger group of Hamiltonians that can be expressed as

$$\hat{H} = \sum_{\mathbf{j}} \sum_{\alpha} h^{\alpha} \hat{S}_{\mathbf{j}}^{\alpha} + \sum_{\langle \mathbf{i}, \mathbf{j} \rangle_{\sigma}} \sum_{\alpha} J_{\sigma}^{\alpha\alpha} \hat{S}_{\mathbf{i}}^{\alpha} \hat{S}_{\mathbf{j}}^{\alpha}, \quad (16)$$

where the second sum includes the bonds of interest. One for us particularly relevant model of this kind is the  $J_1$ - $J_2$  model discussed in the previous subsection;

$$\hat{H}_{J_1 J_2} = J_1 \sum_{\langle \mathbf{i}, \mathbf{j} \rangle} \hat{S}_{\mathbf{i}} \cdot \hat{S}_{\mathbf{j}} + J_2 \sum_{\langle \mathbf{i}, \mathbf{j} \rangle} \hat{S}_{\mathbf{i}}^x \hat{S}_{\mathbf{j}}^x + \hat{S}_{\mathbf{i}}^y \hat{S}_{\mathbf{j}}^y, \quad (17)$$

where  $\hat{S}_{\mathbf{i}} = (\hat{S}_{\mathbf{i}}^x, \hat{S}_{\mathbf{i}}^y, \hat{S}_{\mathbf{i}}^z)$ .

For the classical system comprised of Ising spins  $s = \pm 1$ , the frustration point separates the Néel and striped phases. It is an open debate whether quantum fluctuations can cause a QSL phase in the vicinity of  $J_1 = 2J_2$  [45–48]. The consensus is that indeed an intermediate quantum fluctuation driven phase emerges, and the estimated range for this quantum phase is  $0.42 \lesssim J_2/J_1 \lesssim 0.62$ . Numerical simulations indicate that this is a QSL, either a gaped [45, 46], or a gapless  $\mathbb{Z}_2$  QSL [47], while, a more recent work, using renormalization group arguments, suggests instead that this phase is not a true QSL, but rather a so called *plaquette valence-bond* phase [48].

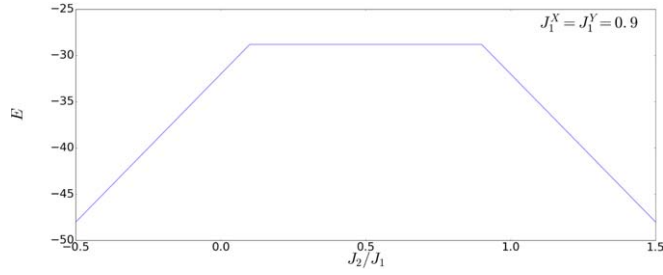


**Figure 5.** The energy of the ground state of the effective Hamiltonian for the Mott insulating phase (9). The energy is found for zero field  $h = 0$ , and for  $J_1^X = J_1^Y = 0.9J_1^Z$ , and as a function of  $J_2^Z/J_1^Z$ . The plot shows that an energy plateau is formed around  $J_2^Z/J_1^Z = 0.5$  indicating the possibility that there is an intermediate phase in between the Néel and striped phases.

Our model, equation (9), is not the full  $J_1$ – $J_2$  model; the NNN couplings between both the  $X$  and  $Y$  terms are absent, and  $J_1^X$ ,  $J_1^Y$ , and  $J_1^Z$  may be different from one another. Nevertheless, the model still holds the promise of yielding phases with novel quantum properties as it supports competing NN and NNN terms. To fully characterize such phases is extremely hard even with state-of-the-art numerical methods. However, already simple methods, like mean-field, can signal the presence of an intermediate phase. To demonstrate this we plot in figure 5 the energy of the ground state of equation (9) as a function of the ratio between NN and NNN coupling amplitudes for zero field  $h = 0$ . While the energy displays an expected constant slope in both the stripe and Néel phase, in an interval around the frustration point the energy stays constant. The range of this interval extends the one predicted for the intermediate quantum phase of the  $J_1$ – $J_2$ -model, but we cannot expect quantitative estimates from simple mean-field methods. However, it is a clear indication that there exists a third phase.

Any anisotropy in the model will induce an effective field in the  $Z$ -direction. It appears already at zeroth order in the perturbation, and hence the field strength  $h$  can to a good approximation be considered as a free parameter [49]. The classical  $J_1$ – $J_2$  composed of Ising spins  $s = \pm 1$  has been analyzed in [50]. The phase diagram is known to consist of four phases; the Néel and striped phases that both survive at zero field  $h = 0$ , the ferromagnetic/polarized phase that appears for sufficiently strong fields  $h$ , and finally a *disordered* phase that only exists for non-vanishing fields. The phase boundaries can be found analytically and when considering classical Ising spins at zero temperature all transitions are first order. The phase diagram for the classical model is depicted in figure 6(a). A most relevant question is how quantum fluctuations, appearing for non-zero  $J_1^X$  and  $J_1^Y$ , will affect the disordered phase. The quantum phase in the interval  $0.42 \lesssim J_2/J_1 \lesssim 0.62$  for  $h = 0$  will only survive moderate fields, and instead some new ‘transverse disordered’ phases will possibly emerge [51–53]. It is by now established that for  $h = 4J_1$  a magnetization plateau (with constant magnetization  $m = 1/2$  per plaquette) establishes due to the order-by-disorder mechanism [51, 52]. This phase has been termed *uuud* (up–up–up–down) to describe the spins for one plaquette. More recently, it has been suggested that a set of additional novel phases may exist for non-zero  $h$ , intervened between the canted (the anti-ferromagnetic phases get canted in the presence of a field) stripe and Néel phases [53]. The nature of such phases is not fully known, but they show characteristics of *supersolids*.

As for figure 5, we explore the case with a non-zero field within the simplest mean-field approach. Adopting the approach of the previous subsection the full system state is factorized between the neighbors, and single site spins are parameterized as  $(\hat{S}_i^X, \hat{S}_i^Y, \hat{S}_i^Z) = (S \sin \theta_i \cos \phi_i, S \sin \theta_i \sin \phi_i, S \cos \theta_i)$ , where  $S = 1/2$  is the spin. This is analogous to assigning spin coherent states to every site. The energy  $E[\theta_i, \phi_i]$  is then numerically minimized with respect to the polar and azimuthal angles  $\theta_i$  and  $\phi_i$  respectively. To distinguish between possible phases we define

$$C_{\text{full}} = \frac{1}{N} \left( \sum_i \langle S_i^Z \rangle + \frac{1}{2} \sum_{\langle i,j \rangle} C^{zz}(\mathbf{i}, \mathbf{j}) + \frac{1}{2} \sum_{\{i,j\}} C^{zz}(\mathbf{i}, \mathbf{j}) \right), \quad (18)$$

what we call the *full correlator* and where, analogous to equation (13),

$$C^{zz}(\mathbf{i}, \mathbf{j}) = \langle S_i^Z S_j^Z \rangle. \quad (19)$$

The full correlator is restricted by  $-1 \leq C_{\text{full}} \leq 1$  and it captures the four classical phases of figure 6(a); the ferromagnetic phase is characterized by  $C_{\text{full}} = 1$ , the Néel phase by  $C_{\text{full}} = 0$ , the striped phase by  $C_{\text{full}} = -1$ , and finally the disordered phase by  $C_{\text{full}} = -1/2$ . The results of such a treatment are presented in figure 6. In (a) we reproduce the classical result [50] up to numerical errors (seen as ‘scatters’ in the vicinities of the phase boundaries). In particular, the four phases mentioned above are clearly visible. As the  $J_1^X$  ( $J_1^Y$ ) becomes

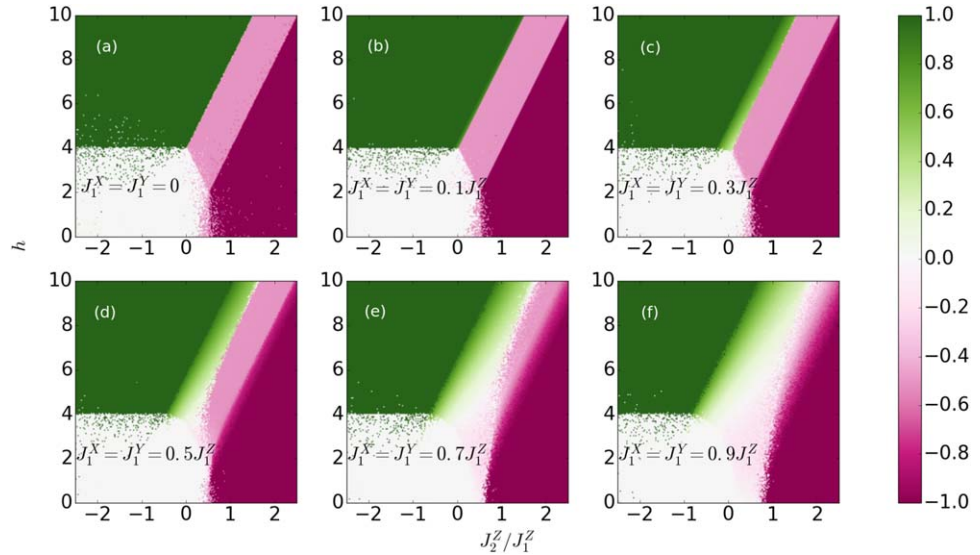


**Figure 6.** The mean-field phase diagram of the model of equation (9), here characterized by the full correlator  $C_{\text{full}}$  defined in (18) and with  $J_1^X = J_1^Y$ . Each plot represents a different coupling strength of  $J_1^X = J_1^Y$  as indicated by the text in the figures. In the case of  $J_1^X = J_1^Y = 0$  we see four distinct phases, the ferromagnetic phase (green), the Néel phase (white), the striped phase (dark pink), and the disordered phase (pink). In this (classical) limit all phase transitions are first order. As we consider non-zero couplings  $J_1^X = J_1^Y$  a fifth mean-field phase appears (light green/pink), this phase grows with increasing couplings  $J_1^X = J_1^Y$ , and all PTs except for the one between the Néel phase and the ferromagnet phase, and the Néel and the new phase, appear to be second order. The new phase survives also for zero field,  $J^Z = 0$ , provided that  $J_1^X = J_1^Y$  is large enough. At this mean-field level, the properties of the intermediate fifth phase is unknown. The dispersed dots are numerical errors for which the simulations are not capable of finding the true ground state.

non-zero the model is no longer integrable and quantum fluctuations set in. The transitions between the disordered phase and the ferromagnetic and striped phases turn continuous. When  $J_1^X$  and  $J_1^Y$  are increased, the size of the classical disordered phase (pink in (a)) is reduced, for the price of a phase reaching down to zero field  $h = 0$  (light pink in (f)). This is what is termed *transverse disordered* in [51]. Our analysis is not capable of distinguishing further properties of this region, e.g. the appearance of the *uuud* phase or other exotic phases [53].

Exact diagonalization is limited to very small lattices which are not capable of extracting long-range correlations. Nevertheless, in figure 7 we compare the mean-field results of  $C_{\text{full}}$  with those of an exact diagonalization for a  $4 \times 4$  lattice. As expected, the finite size effects cause the crossover region between the two anti-ferromagnetic phase to be more extended. However, it still shows a plateau forming in the regime where the mean-field results predicts a new phase, which is again an indicator of a fifth phase.

One last observation of figure 6 regards the extension of the intermediate regime. For a field  $h = 4$ , it seems to survive down to  $J_2^Z/J_1^Z \approx -1$  when  $J_1^X (J_1^Y)$  is of the same order as  $J_1^Z$ . As already mentioned, the nature of this state is unknown, let alone its phase boundaries. The disorder-by-order mechanism will stabilize certain states within this region like the *uuud* phase [51, 52]. To get a better estimate for the phase boundaries more sophisticated methods are needed, but the fact that our mean-field results indicate that something is going on also for negative  $J_2^Z/J_1^Z$  leaves us with hope. Returning to the actual effective model of (9) that describes the Mott insulating phase of our bipartite optical lattice model we note that identically  $J_2^Z/J_1^Z = -1/2$ , and thus we sit on the corresponding vertical line in the phase diagram upon varying  $h$ .

## 4. Conclusion

We have discussed phases of a two dimensional bipartite optical lattices. The feature leading to these novel phases is the alternation between *s*- and *p*-orbital sites. The sites hosting *s*-orbital atoms induces an effective coupling between *p*-orbital atoms, resulting in competing NN and NNN interactions. For effective anti-ferromagnetic coupling terms the system becomes frustrated.

For the Mott insulating phase with a single atom per site, we derive an effective spin-1/2 model for the *p*-orbital atoms. The resulting Hamiltonian is similar to the well known  $J_1$ - $J_2$  model that has been thoroughly studied in the past. As a candidate model for the realization of QSL phases, we discussed the possibilities to find also related frustration driven phases in our system. The mean-field analysis suggested the appearance of a phase whose phase boundaries seemed to qualitatively agree with those of the predicted QSL for the zero field  $J_1$ - $J_2$  model. For a non-vanishing field, which would automatically arise in an anisotropic lattice, a plethora of novel

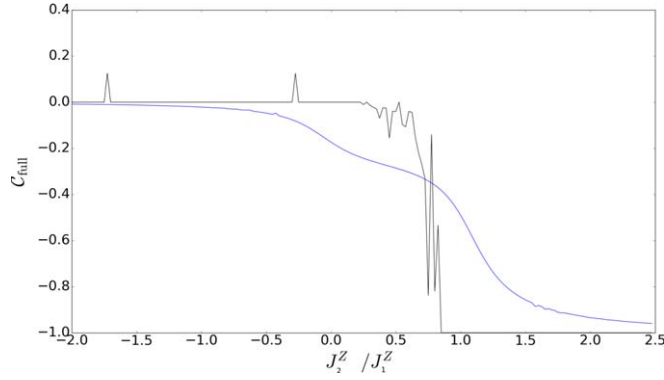


**Figure 7.** The full correlator (18) for zero field  $h$ . The result obtained by mean-field is shown as the black line, while the result from exact diagonalization of a  $4 \times 4$  lattice is represented by the blue line. Remember that for the Néel phase  $C_{\text{full}} = 0$  and in the striped phase  $C_{\text{full}} = -1$ . The range in between these two phases marks the intermediate new phase. For such a small lattice as this, the finite size effects dominate and because of this the exact diagonalization over estimates the intermediate phase. The results of the exact diagonalization indicates that in the intermediate phase a plateau is formed, which hints the presence of a new intermediate phase. The parameters used for this figure are  $J_1^X = J_1^Y = 0.9$ . The sudden jumps of the black line is again numerical artifacts when the code finds a local minima and not the global minimum of the energy functional.

phases have been predicted [53], and we argued that experimentally it might be favorable to actually consider non-zero fields.

In the superfluid phase we also derived an effective model for the  $p$ -orbital atoms, but this time by assuming a large energy detuning between  $s$ - and  $p$ -orbital atomic states. In this regime we can adiabatically eliminate the  $s$ -orbital sites/states. Within this framework we derive a semi-classical model showing great resemblance with a classical XY model. Our system becomes fully frustrated in the anti-ferromagnetic regime, and we discuss whether this could give rise to glass or liquid phases.

To numerically distinguish a true QSL phase from other possible phases is very hard [13]. These are points that would need further investigation, i.e. do we have true QSL phases, and if not what are these phases? And how would they be experimentally probed? As mentioned above, frustration in the SF phase should manifest in time-of-flight measurements. To measure quantum correlations one would need more sophisticated methods like single site detection [54].

## Acknowledgments

We thank Axel Gagne, Themistoklis Mavrogordatos and Andreas Hemmerich for insightful discussions. The Knut and Alice Wallenberg foundation (KAW) and the Swedish research council (VR) are acknowledged for financial support.

## Appendix A. Adiabatic elimination of $s$ -orbital degrees-of-freedom

Under the assumption that  $|\Delta|$  is much larger than the remaining parameters, the  $s$ -orbital atoms will be slaved to the  $p$ -orbital ones. It is then legitimate to adiabatically eliminate the  $s$ -orbital degrees-of-freedom. Following the standard procedure [55], we start from the Heisenberg equations-of-motions as obtained from the full Hamiltonian, equations (2)–(4), to derive

$$\begin{aligned}\partial_t \hat{a}_{\mathbf{i}} &= -i\Delta \hat{a}_{\mathbf{i}} - iU_{ss} \hat{n}_{\mathbf{i}} \hat{a}_{\mathbf{i}} + it_x (\hat{a}_{\mathbf{x}\mathbf{i}+1_x} + \hat{a}_{\mathbf{x}\mathbf{i}-1_x}) + t_y (\hat{a}_{\mathbf{y}\mathbf{i}+1_y} + \hat{a}_{\mathbf{y}\mathbf{i}-1_y}), \\ \partial_t \hat{a}_{\mathbf{x}\mathbf{j}} &= it_x (\hat{a}_{\mathbf{s}\mathbf{j}+1_x} + \hat{a}_{\mathbf{s}\mathbf{j}-1_x}) + \text{interaction terms}, \\ \partial_t \hat{a}_{\mathbf{y}\mathbf{j}} &= it_y (\hat{a}_{\mathbf{s}\mathbf{j}+1_y} + \hat{a}_{\mathbf{s}\mathbf{j}-1_y}) + \text{interaction terms}.\end{aligned}\tag{A.1}$$

Here we have introduced the notation  $\mathbf{i} \pm 1_x$  for the horizontal neighboring sites to site  $\mathbf{i}$ , and  $\mathbf{i} \pm 1_y$  the same but in the vertical direction. The steady state solution for the  $s$ -orbitals is obtained from  $\partial_t \hat{a}_{\mathbf{i}} = 0$ , and we make the further assumption that the  $S$ -sites are initially empty, such that for all times  $\langle \hat{n}_{\mathbf{i}} \rangle \ll 1$  and we neglect the shift deriving from onsite interaction on these sites. The steady state solution then becomes

$$\hat{a}_{\mathbf{i}}^{(ss)} = \frac{t_x}{\Delta} (\hat{a}_{\mathbf{x}\mathbf{i}+1_x} + \hat{a}_{\mathbf{x}\mathbf{i}-1_x}) + \frac{t_y}{\Delta} (\hat{a}_{\mathbf{y}\mathbf{i}+1_y} + \hat{a}_{\mathbf{y}\mathbf{i}-1_y}).\tag{A.2}$$

When substituting this expression for the  $s$ -orbital operators in the equations-of-motion for  $\hat{a}_{\mathbf{x}\mathbf{j}}$  we obtain a series of terms. Apart from the unaffected interaction terms, all of these represent different two-step processes

involving  $p_x$  and  $p_y$  orbital atoms, and hence only operators on the  $\mathcal{P}$ -sites. We write

$$\partial_t \hat{a}_{xj} = \hat{f}_2 + \hat{f}_1, \quad (\text{A.3})$$

where we have divided the terms into different categories. The first

$$\hat{f}_2 = iJ_{2x}(\hat{a}_{xj+2x} + \hat{a}_{xj-2x} + 2\hat{a}_{xj}) \quad (\text{A.4})$$

with (as defined in the main text) the amplitude  $J_{2x} = |t_x|^2 / \Delta$ . Similarly, there are terms describing NN tunneling in the  $\mathcal{P}$ -sublattice, i.e.

$$\hat{f}_1 = iJ_1(\hat{a}_{yj+1_x+1_y} + \hat{a}_{yj+1_x-1_y} + \hat{a}_{yj-1_x+1_y} + \hat{a}_{yj-1_x-1_y}), \quad (\text{A.5})$$

with the amplitude  $J_1 = t_x t_y / \Delta$ . equivalently one finds the corresponding equations for  $\partial_t \hat{a}_{yj}$ . From these equations it is straightforward to derive an effective Hamiltonian for the  $p$ -orbital atoms via

$$\partial \hat{a}_{\alpha j} = -i[\hat{a}_{\alpha j}, \hat{H}_{\text{eff}}]. \quad (\text{A.6})$$

Using the Hamiltonian (7) in the above expression gives the desired equations-of-motion (A.3). The parameter dependence of the coefficients  $J_1$  and  $J_{2\alpha}$  is understood from the types of two-boson processes; a  $p$  orbital atoms tunnels with amplitude  $t_\alpha$  to an  $s$  orbital site, where it acquires an energy contribution  $1/\Delta$ , and finally it tunnels to a  $p$  orbital site with an amplitude  $t_\beta$ . This together gives the coefficient  $t_\beta \left(\frac{1}{\Delta}\right) t_\alpha$ .

## Appendix B. Derivation of the effective Hamiltonian in the Mott phase

The Hamiltonian in the Mott phase is obtained by considering the tunneling part as a perturbation to the full Hamiltonian. Here the fixed number of atoms per lattice site is effectively handled by dividing the Hilbert space of the eigenvalue problem into two orthogonal subspaces using the projection operators  $\hat{P}^2 = \hat{P}$  and  $\hat{Q}^2 = \hat{Q}$  with  $\hat{P} + \hat{Q} = 1$ .  $\hat{P}$  projects onto the subspace  $\mathcal{H}_p$  where all lattice sites are occupied with one atom and  $\hat{Q}$  projects onto the complementary subspace  $\mathcal{H}_Q$ . The eigenvalue problem may be written as

$$\hat{H}(\hat{Q} + \hat{P})\psi = (\hat{H}_K + \hat{H}_U)(\hat{Q} + \hat{P})\psi = E\psi, \quad (\text{B.1})$$

where  $\hat{H}_K$  is the kinetic part of the Hamiltonian, and  $\hat{H}_U$  is the interaction part of the Hamiltonian. This leads to an effective Hamiltonian  $\hat{H}_I$  in the Mott phase with unit filling [49]

$$\hat{H}_I \psi = -\hat{P}\hat{H}_U\hat{Q} \frac{1}{\hat{Q}\hat{H}\hat{Q} - E} \hat{Q}\hat{H}_K\hat{P}\psi. \quad (\text{B.2})$$

This expression is exact and serves as the starting point for treating the tunneling perturbatively, i.e. one expands  $\frac{1}{(\hat{Q}\hat{H}\hat{Q} - E)}$ . Making the approximation  $\frac{1}{\hat{Q}\hat{H}\hat{Q} - E} \approx \frac{1}{\hat{H} - E}$  it follows that

$$\frac{1}{\hat{Q}\hat{H}\hat{Q} - E} \approx \frac{1}{\hat{H}_U} \frac{1}{(1 + \hat{H}_U^{-1}(\hat{H}_K - E))}. \quad (\text{B.3})$$

As the tunneling coefficient is much smaller than the interaction coefficient one may expand around  $\hat{H}_U^{-1}(\hat{H}_K - E)$ . Including terms up to fourth order in the tunneling parameter yields

$$\hat{K} \equiv \frac{1}{\hat{H}_U} \left[ 1 + \frac{1}{\hat{H}_U}(\hat{H}_K - E) + \frac{1}{\hat{H}_U}(\hat{H}_K - E) \frac{1}{\hat{H}_U}(\hat{H}_K - E) \right], \quad (\text{B.4})$$

such that the effective Hamiltonian may be expressed as

$$\hat{H} \sim -t\hat{K}t. \quad (\text{B.5})$$

In any Mott phase only even terms in the expansion will be non-zero. For a bipartite lattice one needs to include fourth order tunneling processes in order to couple two lattice sites of the same type. For a better understanding of these processes, we consider two generic transitions, one starting in an  $\mathcal{S}$ -site, which we label  $\mathcal{C}^S$ , and one starting in a  $\mathcal{P}$ -site denoted  $\mathcal{C}^P$ ;

$$\begin{aligned} \mathcal{C}^P &= t_\alpha t_\beta t_{\alpha'} t_{\beta'} \hat{a}_{\beta_l}^\dagger (\hat{a}_{s_k} \hat{K}_k^S \hat{a}_{s_k}^\dagger) (\hat{a}_{\alpha_j} \hat{K}_l^P \hat{a}_{\beta_j}^\dagger) (\hat{a}_{s_i} \hat{K}_i^S \hat{a}_{s_i}^\dagger) \hat{a}_{\alpha_l}, \\ \mathcal{C}^S &= t_\alpha t_\beta t_{\alpha'} t_{\beta'} \hat{a}_{s_i}^\dagger (\hat{a}_{\alpha_l} \hat{K}_l^P \hat{a}_{\beta_l}^\dagger) (\hat{a}_{s_k} \hat{K}_k^S \hat{a}_{s_k}^\dagger) (\hat{a}_{\alpha_j} \hat{K}_j^P \hat{a}_{\beta_j}^\dagger) \hat{a}_{s_l}. \end{aligned} \quad (\text{B.6})$$

For both processes there are two types of fourth order tunneling processes, those which tunnels out and back along the same path (non-loop processes) and those which makes a loop. In the non-loop process three different lattice sites are involved in the tunneling process, while for loop processes there are four different lattice sites involved. In (B.6) the subscripts  $(i, k)$  refers to  $\mathcal{S}$ -sites and  $(j, l)$  refers to  $\mathcal{P}$ -sites, hence when one is considering a non-loop process two of these will coincide, while for loop processes they will all be different. The full expression for the effective Hamiltonian coming from fourth order transitions is the sum over all possible contributions on

the above form that returns the tunneling atom the original lattice site by the end of the process. The  $\mathcal{S}$ -sites supports only one type of orbital state, the  $s$ -orbital state, as opposed to the  $\mathcal{P}$ -sites which support two orbital states, the  $p_x$  and  $p_y$  states. The one level nature of the  $\mathcal{S}$ -site ensures that the contribution from these sites in the Mott<sub>1</sub> phase will be  $K_{\mathcal{O}}^{\mathcal{S}} = \hat{a}_s^\dagger \hat{a}_s = 1$  for the origin of tunneling process and  $K_{\mathcal{I}}^{\mathcal{S}} = \frac{1}{U_{ss}} \hat{a}_s \hat{a}_s^\dagger = \frac{2}{U_{ss}}$  for an intermediate  $\mathcal{S}$ -site. This allow us to simplify (B.6) as

$$\begin{aligned} C^{\mathcal{S}} &= \frac{2}{U_{ss}} [t_{\alpha_j} t_{\beta_j} (\hat{a}_{\alpha_j} \hat{K}_j^{\mathcal{P}} \hat{a}_{\beta_j}^\dagger)] [t_{\alpha_l}^{\sigma_3} t_{\beta_l}^{\sigma_4*} (\hat{a}_{\alpha_l} \hat{K}_l^{\mathcal{P}} \hat{a}_{\beta_l}^\dagger)], \\ C^{\mathcal{P}} &= \frac{4}{U_{ss}^2} [t_{\alpha_j} t_{\beta_j} \hat{a}_{\beta_j}^\dagger \hat{a}_{\alpha_j}] [t_{\alpha_l}^{\sigma_3} t_{\beta_l}^{\sigma_4*} (\hat{a}_{\alpha_l} \hat{K}_l^{\mathcal{P}} \hat{a}_{\beta_l}^\dagger)]. \end{aligned} \quad (\text{B.7})$$

The interaction between the  $p$ -orbitals  $\hat{K}^{\mathcal{P}}$  depends only on the number of atoms in the lattice site, in the Mott<sub>1</sub> phase there are two atoms in the intermediate lattice sites, and  $\hat{K}^{\mathcal{P}}$  can be written on matrix form

$$\hat{K}^{\mathcal{P}} = \begin{bmatrix} \hat{K}_{xx}^{xx} & \hat{K}_{xx}^{yy} & 0 \\ \hat{K}_{yy}^{xx} & \hat{K}_{yy}^{yy} & 0 \\ 0 & 0 & \hat{K}_{xy}^{xy} \end{bmatrix}, \quad (\text{B.8})$$

where

$$\hat{K}_{\alpha\alpha}^{\alpha\alpha} = 2 \frac{U_{\beta\beta}}{U^2}, \quad \hat{K}_{\alpha\beta}^{\alpha\beta} = \frac{1}{U_{xy}}, \quad \hat{K}_{\alpha\alpha}^{\beta\beta} = -4 \frac{U_{xy}}{U^2} \hat{a}_{\beta}^\dagger \hat{a}_{\beta}^\dagger \hat{a}_{\alpha} \hat{a}_{\alpha}, \quad (\text{B.9})$$

with  $U^2 = U_{xx} U_{yy} - U_{xy}^2$  [49]. More compactly one may define the contributing  $\mathcal{P}$ -sites in terms of four different processes depending on if the transition has a loop or non-loop structure, and depending if the  $\mathcal{P}$ -site is the origin ( $\mathcal{O}$ ) or an intermediate site ( $\mathcal{I}$ ) in the process;

$$\begin{aligned} \hat{T}_O^{\sigma} &= \sum_{\alpha\alpha'} t_{\alpha'}^{\sigma*} t_{\alpha}^{\sigma} \hat{a}_{\alpha'}^\dagger \hat{a}_{\alpha}, & \hat{T}_I^{\sigma} &= \sum_{\alpha\alpha'} t_{\alpha'}^{\sigma*} t_{\alpha}^{\sigma} \hat{a}_{\alpha'} \hat{K}_I^{\mathcal{P}} \hat{a}_{\alpha}^\dagger, \\ \hat{L}_O^{\sigma\sigma'} &= \sum_{\alpha\alpha'} t_{\alpha'}^{\sigma*} t_{\alpha}^{\sigma'} \hat{a}_{\alpha'}^\dagger \hat{a}_{\alpha}, & \hat{L}_I^{\sigma\sigma'} &= \sum_{\alpha\alpha'} t_{\alpha'}^{\sigma*} t_{\alpha}^{\sigma'} \hat{a}_{\alpha'} \hat{K}_I^{\mathcal{P}} \hat{a}_{\alpha}^\dagger. \end{aligned} \quad (\text{B.10})$$

For non-loop ( $\hat{T}$ ) the tunneling takes place out and back along the same path, and there is only one superscript  $\sigma$ , while for loops the tunneling out and back into a lattice site are along two different bonds. In total we may distinguish between four different tunneling processes. Two which starts in an  $\mathcal{P}$  site, where one of them will be loop ( $\hat{C}_L^{\mathcal{P}}$ ) and one will be a non-loop ( $\hat{C}_T^{\mathcal{P}}$ ), and two which start in an  $\mathcal{S}$ -site, with similar structure. Then (B.7) may be expressed in terms of (B.10)

$$\begin{aligned} \hat{C}_T^{\mathcal{S}} &= \frac{2}{U_{ss}} \hat{T}_{I_j}^{\sigma} \hat{T}_{I_l}^{\sigma}, & \hat{C}_L^{\mathcal{S}} &= \frac{4}{U_{ss}^2} \hat{L}_{I_j}^{\sigma\sigma'} \hat{L}_{I_l}^{\sigma}, \\ \hat{C}_T^{\mathcal{P}} &= \frac{2}{U_{ss}} \hat{T}_{O_j}^{\sigma} \hat{T}_{I_l}^{\sigma}, & \hat{C}_L^{\mathcal{P}} &= \frac{4}{U_{ss}^2} \hat{L}_{O_j}^{\sigma\sigma'} \hat{L}_{I_l}^{\sigma}. \end{aligned} \quad (\text{B.11})$$

Summing over neighboring pairs of  $\mathcal{P}$ -sites connected via a loop or a non-loop transition then leads to an effective Hamiltonian of the form (9). Using (B.9) the coupling constants may be evaluated. In the isotropic lattice  $h = 0$ , and  $J^Z$ ,  $J^X$  and  $J^Y$  are given by

$$\begin{aligned} J^X &= 4t^4 \left[ \frac{V - \gamma}{U_{ss}^2} - \frac{(V - \gamma)^2}{U_{ss}} \right], \\ J^Y &= 4t^4 \left[ \frac{V + \gamma}{U_{ss}^2} + \frac{(V + \gamma)^2}{U_{ss}} \right], \\ J^Z &= 2t^4 \left[ \frac{4V_z}{U_{ss}^2} + \frac{V_z^2}{U_{ss}} \right], \end{aligned} \quad (\text{B.12})$$

with  $V = 120U_{xy}/U^2$ ,  $\gamma = 1/U$  and  $V_z = 4\tilde{U}/U^2 + 1/(2U_{xy})$ , and where  $U_{xx} = U_{yy} = U$  and  $\tilde{U} = U^2 - U_{xy}^2$ . In the harmonic approximation, where  $U_{xx} = U_{xy} = 3U_{xy}$ , the coupling coefficients

$$\begin{aligned}
J^x &= \frac{52t^4}{U_{xy}U_{ss}} \left[ \frac{1}{U_{ss}} - \frac{13}{U_{xy}} \right], \\
J^y &= \frac{4 \cdot 41t^4}{3U_{xy}U_{ss}} \left[ \frac{1}{U_{ss}} + \frac{41}{3U_{xy}} \right] \approx \frac{56t^4}{U_{ss}U_{xy}} \left[ \frac{1}{U_{ss}} + \frac{14}{U_{xy}} \right], \\
J^z &= \frac{16\sqrt{2} + 9}{9} \frac{t^4}{U_{xx}U_{yy}} \left[ \frac{4}{U_{ss}} + \frac{16\sqrt{2} + 9}{18U_{xy}} \right] \approx \frac{16t^4}{U_{ss}U_{xy}} \left[ \frac{1}{U_{ss}} + \frac{1}{U_{xy}} \right].
\end{aligned} \tag{B.13}$$

## References

- [1] Lewenstein M, Sanpera A, Ahufinger V, Damski B, Sen(De) A and Sen U 2007 *Adv. Phys.* **56** 243  
Bloch I, Dalibard J and Zwerger W 2008 *Rev. Mod. Phys.* **80** 885  
Zoller P and Gardiner C W 2017 *The Quantum World Of Ultra-cold Atoms And Light—Book III: Ultra-Cold Atoms* (Singapore: World Scientific)
- [2] Bloch I, Dalibard J and Naschimbene S 2012 *Nat. Phys.* **8** 267  
Cirac J I and Zoller P 2012 *Nat. Phys.* **8** 264  
Hauke P, Cucchietti F M, Tagliacozzo L, Deutsch I and Lewenstein M 2012 *Rep. Prog. Phys.* **75** 082401
- [3] Jaksch D and Zoller P 2005 *Ann. Phys.* **315** 52
- [4] Jaksch D, Bruder C, Cirac J I, Gardiner C W and Zoller P 1998 *Phys. Rev. Lett.* **81** 3108
- [5] Greiner M, Mandel O, Esslinger T, Hänsch T W and Bloch I 2002 *Nature* **415** 39
- [6] Isacsson A and Girvin S M 2005 *Phys. Rev. A* **72** 053604
- [7] Wu C, Liu W V, Moore J and Sarma D S 2006 *Phys. Rev. Lett.* **97** 190406  
Wu C and Sarma D S 2008 *Phys. Rev. B* **77** 235107  
Wu C 2008 *Phys. Rev. Lett.* **101** 186807  
Larson J, Collin A and Martikainen J-P 2009 *Phys. Rev. A* **79** 033603
- [8] Duan L M, Demler E and Lukin M D 2003 *Phys. Rev. Lett.* **91** 090402
- [9] Pinheiro F, Martikainen J-P and Larson J 2012 *Phys. Rev. A* **85** 033638
- [10] Müller T, Fölling S, Widera A and Bloch I 2007 *Phys. Rev. Lett.* **99** 200405
- [11] Simon J, Bakr W S, Ma R, Tai M E, Preiss P M and Greiner M 2011 *Nature* **473** 307
- [12] Moessner R and Sondhi L 2001 *Phys. Rev. B* **63** 224401  
Powell B J and McKenzie R H 2011 *Rep. Prog. Phys.* **75** 056501
- [13] Balents L 2010 *Nature* **464** 199  
Zhou Y, Kanoda K and Ng T-K 2017 *Rev. Mod. Phys.* **89** 025003
- [14] Nayak C, Simon S H, Stern A, Freedman M and Das-Sarma S 2008 *Rev. Mod. Phys.* **80** 1083
- [15] Struck J, Ölschläger C, Le Targat R, Soltan-Panahi P, Eckhardt A, Lewenstein M, Windpassinger P and Sengstock K 2011 *Science* **333** 996
- [16] Eckhardt A, Hauke P, Soltan-Panahi P, Becker C, Sengstock K and Lewenstein M 2010 *Europhys. Lett.* **89** 10010
- [17] Wirth G, Ölschläger M and Hemmerich A 2011 *Nat. Phys.* **7** 147
- [18] Ölschläger M, Wirth G, Kock T and Hemmerich A 2012 *Phys. Rev. Lett.* **108** 075302
- [19] Cai Z and Wu C 2011 *Phys. Rev. A* **84** 033635
- [20] Li X, Paramakanti A, Hemmerich A and Liu W V 2014 *Nat. Commun.* **5** 3205
- [21] Larson J and Martikainen J P 2012 *Phys. Rev. A* **86** 023611
- [22] Collin A, Larson J and Martikainen J P 2010 *Phys. Rev. A* **81** 023605  
Sowinski T, Lacki M, Dutta O, Pietraszewicz J, Sierant P, Gajda M, Zakrzewski J and Lewenstein M 2013 *Phys. Rev. Lett.* **111** 215302
- [23] Zhou X, Li Y, Cai Z and Wu C 2013 *J. Phys. B: At. Mol. Opt. Phys.* **46** 249501
- [24] Auerbach A 1994 *Interacting Electrons and Quantum Magnetism* (New York: Springer)
- [25] Roscilde T, Verrucchi P, Fubini A, Haas S and Tognetti V 2005 *Phys. Rev. Lett.* **94** 147208
- [26] In the superfluid phase the mean-field ansatz is surprisingly accurate, it gives quantitative description already for 5-10 atoms/site;  
Collin A, Larson J and Martikainen J-P 2010 *Phys. Rev. A* **81** 023605
- [27] Sachdev S 2013 *Quantum Phase Transitions* 1st edn (Cambridge: Cambridge University Press)
- [28] Wikberg E, Larson J, Bergholtz E J and Karlhede A 2012 *Phys. Rev. A* **85** 033607
- [29] Scarola V W and Das Sarma S 2005 *Phys. Rev. Lett.* **95** 033003
- [30] Henley C L 1989 *Phys. Rev. Lett.* **62** 2056  
Prakash S and Henley C L 1990 *Phys. Rev. B* **42** 6574
- [31] Jiang H-C, Yao H and Balents L 2012 *Phys. Rev. B* **86** 024424
- [32] Chitra R, Pati S, Krishnamurthy H R, Sen D and Ramasesha S 1995 *Phys. Rev. B* **52** 6581  
Chen S, Wang L, Gu S J and Wang Y 2007 *Phys. Rev. E* **76** 061108
- [33] Villain J 1977 *J. Phys. C: Solid State Phys.* **10** 1717
- [34] Teitel S and Jayaprakash C 1983 *Phys. Rev. B* **27** 598  
Teitel S and Jayaprakash C 1983 *Phys. Rev. Lett.* **51** 1999
- [35] Berge B, Diep H T, Ghazali A and Lallemand P 1985 *Phys. Rev. B* **34** 3177  
Lee J, Kosterlitz J M and Granato E 1991 *Phys. Rev. B* **43** 11531(R)  
Ramirez-Santiago G and Jose J V 1994 *Phys. Rev. B* **49** 9567  
Lee S and Lee K-C 1994 *Phys. Rev. B* **49** 1518  
Olsson P 1995 *Phys. Rev. Lett.* **75** 2758  
Luo H J, Schülke L and Zheng B 1998 *Phys. Rev. Lett.* **81** 180  
Hasenbusch M, Pelissetto A and Vicare E 2005 *J. Stat. Mech.* **P12002**
- [36] Henley C L and Prakash S 1988 *J. Phys. Colloques* **49** 1197

- [37] Read N and Sachdev S 1991 *Phys. Rev. Lett.* **66** 1773
- [38] Chandra P and Doucot B 1988 *Phys. Rev. B* **38** 9335 R
- [39] Kalz A, Honecker A and Moliner M 2011 *Phys. Rev. B* **84** 174407  
Jin S, Sen A and Sandvik A W 2012 *Phys. Rev. Lett.* **108** 045702  
Ramazanov M K, Murtazaev A K and Magomedov M A 2016 *Solid State Commun.* **233** 35
- [40] Nightingale M P 1977 *Phys. Lett. A* **59** 486  
Binder K and Landau D P 1980 *Phys. Rev. B* **21** 1941
- [41] Villain J, Bidaux R, Carton J P and Conte R 1980 *J. Phys.* **41** 1263
- [42] Kawamura H and Tanemura M 1987 *Phys. Rev. B* **36** 7177
- [43] Sorokin A O and Syromyatnikov A V 2012 *Phys. Rev. B* **85** 174404
- [44] Bergman D, Alicea J, Gull E, Trebst S and Balents L 2007 *Nat. Phys.* **3** 487
- [45] Jiang H-C, Yao H and Balents L 2012 *Phys. Rev. B* **86** 024424
- [46] Wang L and Sandvik A W 2018 *Phys. Rev. Lett.* **121** 107202
- [47] Hu W J, Becca F, Parola A and Sorella S 2013 *Phys. Rev. B* **88** 060402(R)
- [48] Gong S S, Zhu W, Sheng D N, Motrunich O I and Fisher M P A 2014 *Phys. Rev. Lett.* **113** 027201
- [49] Pinheiro F, Bruun G M, Martikainen J P and Larson J 2013 *Phys. Rev. Lett.* **111** 205302
- [50] Slotte P A 1983 *J. Phys. C: Solid State Phys.* **16** 2935
- [51] Zhitomirsky M E, Honecker A and Petrenko O A 2000 *Phys. Rev. Lett.* **85** 3269
- [52] Coletta T, Zhitomirsky M E and Mila F 2013 *Phys. Rev. B* **87** 060407(R)
- [53] Morita K and Shibata N 2016 *J. Phys. Soc. Japan* **85** 094708
- [54] Sherson J F, Weitenberg C, Endres M, Cheneau M, Bloch I and Kuhr S 2010 *Nature* **467** 68
- [55] Gardiner C W and Zoller P 2014 *The Quantum World of Ultra-Cold Atoms and Light Book I: Foundations of Quantum Optics* (Singapore: World Scientific)